Crystal structures of new potassium silicates and aluminosilicates of Sm, Tb, Gd, and Yb and their relation to the armstrongite (CaZr(Si₆O₁₅)·3H₂O) structure

Vladimir K. Taroev [a,b], Anvar A. Kashaev [c], Thomas Malcherek [d], Joerg Goettlicher [e,*], Ekaterina V. Kaneva [a], Alexander D. Vasiljev [f], Ludmila F. Suvorova [a], Daria S. Suvorova [c], Vladimir L. Tauson [a]

[a] A.P. Vinogradov Institute of Geochemistry, Siberian Branch of R.A.S., 1a Favorski Street, Irkutsk 664033, Russia
[b] National Research Irkutsk State Technical University, 83 Lermontov Street, Irkutsk 664054, Russia
[c] Institute of Earth Crust, Siberian Branch of R.A.S., 128 Lermontov Street, Irkutsk 664054, Russia
[d] Mineralogisch-Petrographisches Institut, Universität Hamburg, Grindelallee 48, 20146 Hamburg, Germany
[e] Karlsruhe Institute of Technology, ANKA Synchrotron Radiation Facility, 76344 Eggenstein-Leopoldshafen, Germany
[f] L.V. Kirensky Institute of Physics, Siberian Branch of R.A.S., 50/38 Akademgorodok Street, Krasnoyarsk 660036, Russia

ARTICLE INFO

ABSTRACT

Silicates of composition $K_{7.81}Sm_3Si_{12}O_{32}(OH)_{0.81} \cdot 0.77H_2O$ and $K_7Tb_3Si_{12}O_{32} \cdot 1.36H_2O$, with the space group $P\bar{1}$ and unit cell parameters of $a=6.9218(3)$, $b=11.4653(4)$, $c=11.6215(4)$ Å, $\alpha=88.063(3)°$, $\beta=88.449(3)°$, $\gamma=79.266(3)°$ and $a=6.872(3)$, $b=11.440(5)$, $c=11.542(6)$ Å, $\alpha=88.19(4)°$, $\beta=88.86(4)°$, $\gamma=79.65(4)°$, respectively, were synthesized under hydrothermal conditions. Both crystal structures were determined from twinned crystals, and can be idealized to a composition of $K_7Ln_3Si_{12}O_{32}$ $(KOH)_x(H_2O)_{(2-x)}$ (Ln=Sm, Tb), which is closely related to $K_8Nd_3Si_{12}O_{32}(OH)$. Crystals of the aluminosilicates $K_2GdAlSi_4O_{12} \cdot 0.25H_2O$ and $K_2SmAlSi_4O_{12} \cdot 0.375H_2O$ prepared by the same method possess monoclinic symmetry with the space group $C2/c$. The corresponding unit cell parameters are: $a=26.67(1)$, $b=7.294(3)$, $c=14.835(6)$ Å, $\beta=123.44(3)°$; and $a=26.7406(9)$, $b=7.3288(2)$, $c=14.8498(6)$ Å, $\beta=123.514(1)°$, respectively. A new type of silicate anion that forms tubes was detected in the $K_4Yb_2Si_8O_{21}$ structure. $K_4Yb_2Si_8O_{21}$ is of monoclinic symmetry with the space group $C2/c$. The unit cell parameters are: $a=17.440(2)$, $b=11.786(1)$, $c=12.802(2)$ Å, and $\beta=130.902(1)°$. The structure is a mixed framework of tubes formed by silica-oxygen tetrahedra connected by pairs of edge sharing Yb-octahedra. The relation of the silicate layers and frameworks encountered in these compounds to the armstrongite silicate framework is discussed.

© 2015 Elsevier Inc. All rights reserved.

1. Introduction

A systematic research on rare-earth silicates that can be formed in nature under hydrothermal alteration of granitic or alkaline rocks is of importance to geochemistry. Such mineral phases possibly have an effect on the *REE* distribution often used for the genetic interpretation of magmatic and post-magmatic processes. On the other hand, *REE* silicates belong to a multifunctional group of materials with a permanently increasing scope of applications. These substances are of practical interest due to their valuable physical properties and particularly their luminescent, laser, piezo-electric, and ferroelectric properties. Consequently syntheses and structural investigations of *REE* silicates currently are important

not only for the interpretation of mechanisms of geological processes but also to the preparation of new functional materials.

2. Materials and method of synthesis

This study presents crystal structures of phases obtained in the system SiO_2–Al_2O_3–REE_2O_3–KOH–H_2O, where REE=Yb, Sm, Tb, or Gd. Hydrothermal synthesis was carried out in an autoclave made of stainless steel and equipped with either copper or nickel containers – sealed by argon arc welding before the experiments – at a total pressure of 100 MPa in aqueous alkaline solution with a concentration of KOH=15.25 wt%. Use of containers made of Cu and Ni maintain the oxygen fugacity at a constant level, which is particularly important to elements with variable valence, as is the case for some *REE*. The temperature (500 °C) in the experiments

that lasted 30 days was maintained at $\pm 5\,°C$ for many days with the temperature drift considered. The oxides SiO_2, Al_2O_3, and Yb_2O_3, Sm_2O_3, Tb_2O_3, Gd_2O_3 at a molar ratio $SiO_2/Al_2O_3 = 11.21$ were used as the initial charge. All chemicals were of analytical grade and used as received. Silica and alumina were finely dispersed powders that consisted of amorphous SiO_2 and mainly corundum (α-Al_2O_3), respectively. After operating the autoclaves under steady state conditions, they were quenched in cold running water. The method of synthesis under hydrothermal conditions was reported in detail in [1]. Under these conditions and with the addition of oxides of Yb, Sm, Tb, and Gd to the system of KOH–Al_2O_3–SiO_2–H_2O new or rarely studied potassium *REE* (Al)SiO-compounds might be expected.

Previously, the method was applied to the system KOH–Eu_2O_3–SiO_2–H_2O where Eu-containing silicates were synthesized under different oxygen fugacities [2]. In another study, a new type of HK_6Eu^{3+} [$Si_{10}O_{25}$] silicate was identified with a new structural unit consisting of nano-scale tubes based on eight-fold rings of silicate tetrahedra [3].

3. Equipment and methods to study synthesized phases

Element composition of the synthesized phases was determined with a JEOL JXA-8200 electron microprobe, equipped with a scanning electron microscope, an energy-dispersive Si(Li) detector of 133 eV resolution, and five spectrometer crystals for wave length dispersive analysis.

The latter was used to determine the chemical composition of the synthesized crystals and inclusions. The conditions of excitation and registration of analytical signals are as follows: Accelerating voltage 20 kV, current of probe 20 nA, diameter of electron beam 1–10 μm, depending on the size of the analyzed crystal. Concentrations were calculated by the ZAF-method and calibrated by natural minerals and synthetic compounds certified as laboratory reference samples at the Institute of Geology and Mineralogy SB RAS in Novosibirsk: Orthoclase—for K, Al, Si; Gd_2O_3—for Gd; $LiSmMoO_4$—for Sm; Yb_2O_3 for—Yb; metallic Tb—for Tb. The chemical formulas of the synthesized *REE* silicates derived from electron probe micro-analysis results are provided in Table 1.

Crystal structures were studied with a Nonius KappaCCD single-crystal diffractometer. A combination of φ and ω scans was used to collect full reflection spheres. Diffraction maxima were indexed using the φ/ψ-method and the DirAx program [4]. Integration and correction of intensity data were carried out using the Eval-14 procedures [5] as implemented in the EvalCCD software package. Diffraction data for the KSm silicate were integrated and corrected using Eval15 [6]. Structures were solved using Sir 92/Wingx [7] and completed by inspection of difference Fourier maps. Structure refinement was performed using Jana2006 [8]. The $K_4Yb_2Si_8O_{21}$ crystal structure was studied using a SMART APEX II single-crystal diffractometer with CCD detector (Bruker AXS). All diffraction data were collected with Mo$K\alpha$-radiation passed through a graphite monochromator. The absorption corrections were obtained with the SADABS program [9]. The structure of $K_4Yb_2Si_8O_{21}$ was solved by direct methods and refined in anisotropic approach for non-hydrogen atoms using the SHELXTL program [10].

4. Results and discussion

4.1. KSm and KTb silicates

The KSm and KTb crystals are twinned about the normal to (0 0 1). The chemical composition obtained from structure refinement and electron microprobe analysis and the structure characteristics of crystals are given in Table 1. The crystal structures of these two phases are quite similar. They belong to the group of open-branched single-layer silicates [11] with mixed tetrahedral–octahedral frameworks.

Silicate tetrahedra form layers parallel to (1 1 0) for both the KSm and the KTb silicates. Two types of six-membered rings as well as eight- and twelve-membered rings of corner-sharing tetrahedra can be identified within these layers (Fig. 1). The layers are connected by isolated as well as by edge-sharing pairs of SmO_6-octahedra, while K ions and water molecules occupy the structural cavities. The crystal structure of KSm silicate along the *a* axis is shown in Fig. 2 and final atomic coordinates are reported in Table 2.

Single octahedra show slight deviations from the ideal form with $\langle Sm1–O \rangle = 2.325(3)$ and $\langle Tb1–O \rangle = 2.291(7)$ Å for KSm and KTb silicate, respectively. Angles O–Sm1–O deviate from $90°$ by not more than $5.78°$ with $180°$ for the diametrically opposed O atoms, the edge lengths vary in the range of 3.164–3.452 Å. For diametrically opposed oxygen atoms, the values of O–Tb1–O angles are 157.5, 166.3, and $171.4°$ instead of the ideal value of $180°$.

Sm2-octahedra in KSm silicate are distorted by the mutual repulsion of the Sm atoms. The length of the shared edge is 2.770(6) Å and $\langle Sm2–O \rangle = 2.334(48)$ Å, with distances to the oxygen atoms of the edge being 2.402(4) and 2.381(4) Å. Deviations of O–Sm2–O angles from the ideal values are significantly higher than in the Sm1 octahedron. For these diametrically opposed oxygen atoms the values of the angles are $166.3°$, $155.7°$ and $170.2°$ compared to the ideal value of $180°$. The Tb2-octahedra in KTb silicate are also distorted. The averaged length Tb2–O = 2.298(45) Å with the distances to the oxygen atoms of the edge being equal to 2.353 and 2.374 Å. The length of octahedron shared edge O–O is 2.783 Å. The average bridging Si–O–Si angles in KSm and KTb silicate structures are $142.3°$ and $131.6°$, respectively. The bond lengths in the SiO_4-tetrahedra are distorted, because one part of the oxygen atoms is connected with the Si atoms only, while the other is connected with the Sm or Tb atoms as well. The lengths of the Si–O bonds of the second type are shortened due to the greater impact of the Si atoms on them. In fact, the shortened average length in KSm silicate structure is 1.576 Å with $\langle Si–O \rangle = 1.618$ (24) Å. The silicate tetrahedra in the KTb structure have the same average bond lengths as for KSm-silicate.

The well-ordered K1 and K2 atoms in the KSm silicate structure are surrounded by seven framework oxygen anions with K–O distances in the range from 2.748 to 3.356 and from 2.731 to 3.366 Å, respectively. Other K atoms (K31, K32, K41, K42, Kc1) are located in partly occupied positions. Further oxygen atoms Oc1, Oc2, and Oc3 are attributed to H_2O and OH-groups and partly fill the voids in the structural channels formed by the eight-membered silicate rings. Considering bond valence calculations, Oc1 is most likely to be occupied by water molecules, while Oc2 and Oc3 have a larger preference for $(OH)^-$, as these oxygen atoms receive stronger bond valence contributions from K-cations. The thermal displacement parameters of these atoms were constrained to the same isotropic value in the structure refinement taking the disordered nature of their positions into account. The associated hydrogen positions remain undetermined. The split channel site K_{c1} is mainly occupied by K^+. This can be inferred from its scattering power, which would otherwise require an implausible O-occupation in significant excess of 50%. The observed difference in K-content between the X-ray structure ($K_{7.814}Sm_3Si_{12}O_{32}(OH)_{0.814} \cdot 0.77H_2O$) and electron microprobe analysis ($K_{6.892}Sm_{3.076}Si_{11.97}O_{32}$) (Table 1) can be attributed entirely to these extra-framework K-atoms. As the two compositions were determined using different crystals, these differences reflect the inhomogeneity and disorder of the channel contents in these compounds. An idealized composition $K_7Sm_3Si_{12}O_{32}(KOH)_x(H_2O)_{(2-x)}$ can be formulated to accommodate the additional K-content. K may be underestimated by the electron microprobe because of its higher volatility as compared to Si.

Table 1
Characterization of crystals and results of structure refinements of K-silicates of Sm, Tb and Yb and K-aluminosilicates of Gd and Sm.

|	KSm-silicate	KTb-silicate	KGd-aluminosilicate	KSm-aluminosilicate	KYb-silicate
Composition from structure refinement	$K_{7.814}Sm_3Si_{12}O_{32}(OH)_{0.814} \cdot 0.77H_2O$	$K_{7.04}Tb_3Si_{12}O_{32.02} \cdot 1.36H_2O^e$	$K_2GdAlSi_4O_{12} \cdot 0.25H_2O$	$K_2SmAlSi_4O_{12} \cdot 0.375H_2O$	$K_4Yb_2Si_8O_{21}$
Composition from electron microprobe analysis	$K_{6.892}Sm_{3.07}Si_{11.97}O_{32}{}^a$	$K_{6.97}Tb_{2.83}Si_{12}O_{31.73} \cdot 1.36H_2O^b$	$K_{2.02}Gd_{0.96}Al_{0.96}Si_{4.04}O_{11.98} \cdot 0.25 H_2O^{b,c}$	$K_{1.99}Sm_{0.97} Al_{1.06}Si_{3.94} O_{11.91} \cdot 0.375H_2O^{bc}$	$K_{3.97}Yb_{1.93}Si_8O_{20.89}{}^d$
Crystal system	Triclinic	Triclinic	Monoclinic	Monoclinic	Monoclinic
Space group	$P\bar{1}$	$P\bar{1}$	$C2/c$	$C2/c$	$C2/c$
a (Å)	6.9218(3)	6.872(3)	26.67(1)	26.7406(9)	17.440(2)
b (Å)	11.4653(4)	11.440(5)	7.294(3)	7.3288(2)	11.786(1)
c (Å)	11.6215(4)	11.542(6)	14.835(6)	14.8498(4)	12.802(2)
α (°)	88.063(3)	88.19(4)	90	90	90
β (°)	88.449(3)	88.86(4)	123.44(3)	123.514(1)	130.902(1)
γ (°)	79.266(3)	79.65(4)	90	90	90
V (Å^3)	905.43(6)	892.1(8)	2408(2)	2426.4(1)	1988.9(4)
θ_{max}(°)	33	34.99	35.05	34.91	29.54
μ (mm^{-1})	6.19	7.2	6.73	6.06	10.77
Z	1	1	8	8	4
N unique reflections for $I > 3\sigma (I)$	3419	3442	4585	4644	2306
N (all reflections)	4632	4513	5293	5308	2508
N (Parameters)	264	260	210	188	160
R (all reflections)	0.0591	0.0691	0.0297	0.0267	0.023
R ($I > 3\sigma (I)$)	0.0373	0.0445	0.0234	0.0212	0.02
δ_{max} (e/Å^3)	1.77	2.04	1.29	1.01	0.930
δ_{min} (e/Å^3)	-1.00	-1.80	-0.90	-1.03	-1.137

[a] Normalized to 32 anions.
[b] Normalized to water content obtained from structure refinement.
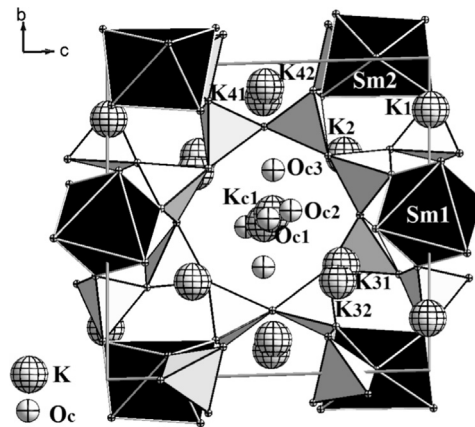[c] Normalized to Al+Si=5.
[d] Normalized to Si=8.
[e] Or $K_{7.04}Tb_3Si_{12}O_{32}(OH)_{0.04} \cdot 1.32H_2O$ to be compatible with the KSm silicate.
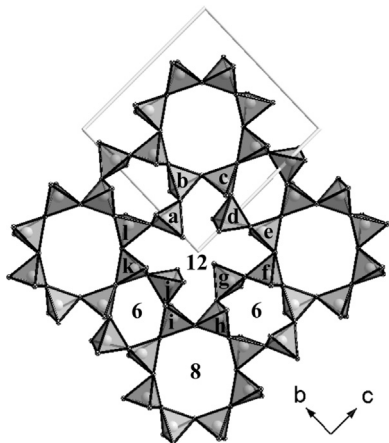
Fig. 1. The $S_{12}O_{32}$ layer in KSm and KTb silicates projected along [1 0 0]. Six-, eight-, and twelve-membered rings are indicated.

Fig. 2. The crystal structure of $K_{7.81}Sm_3Si_{12}O_{32}(OH)_{0.81} \cdot 0.77H_2O$ projected down the a axis. Sm-polyhedra are shown in black, Si-tetrahedra are colored white/gray.

In the structure of KTb-containing silicate, the shape of the K2 polyhedron is somewhat different in so far as it has eight apexes. K1–O bond lengths vary within 2.745–3.761 and K2–O within 2.725–3.365 Å. There are some uncertainties relating to the detection and localization of OH/H$_2$O and potassium atoms. Both structures (K$_{7.814}$Sm$_3$ Si$_{12}$O$_{32}$(OH)$_{0.814}$ · 0.77H$_2$O and K$_7$Tb$_3$Si$_{12}$O$_{32}$ · 1.36H$_2$O) were refined with varying degree of disorder involving K and H$_2$O. Due to this disorder, no hydrogen atoms could be located and H$_2$O was entirely represented by its central oxygen atom in the structure models used. The KSm-silicate appears to host additional K-atoms inside its channels, which have to be charge balanced by extra-framework (OH)$^-$ anions also situated inside these channels. Only water and very little K were identified in the center of the channels of the KTb-silicate.

A very similar structure was described in reference [12] albeit with higher water content per formula unit, K$_7$Sm$_3$Si$_{12}$O$_{32}$ · 3H$_2$O. Structures of KSm- and KTb-silicates also are very similar to the previously described K$_7$Eu$_3$Si$_{12}$O$_{32}$ · 4H$_2$O [12], K$_8$Nd$_3$Si$_{12}$O$_{32}$(OH) [13], K$_{8-x}$[Yb$_3$Si$_{12}$O32](OH)$_{1-x}$ · H$_2$O [14], K$_9$Y$_3$Si$_{12}$O$_{32}$F$_2$ [15], and K$_8$Gd$_3$Si$_{12}$O$_{32}$Cl · 2H$_2$O [16]. Differences are restricted to the occupancy of the structural channels.

4.2. KGd and KSm aluminosilicates

KGd aluminosilicate crystals were synthesized using nickel containers. The structure of this compound is quite close to that of a similar compound synthesized in Cu-containers. The space group was determined to be $C2/c$ (Table 1) because no violations of

Table 2
Relative coordinates and equivalent thermal parameters of atoms in the structure of $K_{7.814}Sm_3Si_{12}O_{32}(OH)_{0.814} \cdot 0.77H_2O$.

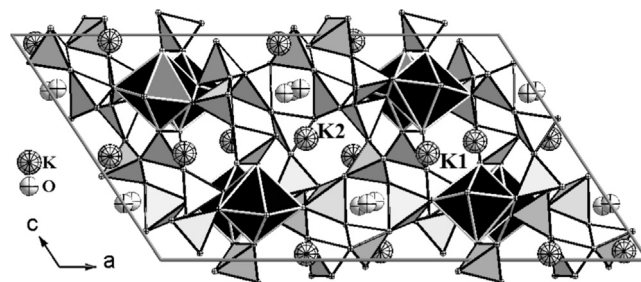| Atom	x	y	z	U_{eq}	Occupancy
Sm1	0	0.5	0	0.0110(1)	1
Sm2	0.51039(4)	0.01171(3)	0.16662(2)	0.01044(8)	1
Si1	0.3150(2)	−0.1967(1)	0.3479(1)	0.0121(4)	1
Si2	0.6948(3)	0.1762(2)	0.3786(1)	0.0132(5)	1
Si3	0.3366(2)	0.5961(1)	0.1938(1)	0.0106(4)	1
Si4	0.6556(2)	0.3658(1)	0.1863(1)	0.0108(4)	1
Si5	0.0105(2)	0.0113(1)	0.2518(1)	0.0117(4)	1
Si6	0.5491(2)	0.7348(1)	0.0099(1)	0.0097(4)	1
O1	0.7638(6)	0.6675(4)	0.0362(4)	0.016(1)	1
O2	0.5218(7)	0.1155(4)	0.3368(4)	0.021(1)	1
O3	0.4957(7)	−0.1487(4)	0.2895(4)	0.019(1)	1
O4	0.9115(7)	0.0936(4)	0.3602(4)	0.023(1)	1
O5	0.8444(6)	−0.0070(4)	0.1652(4)	0.022(1)	1
O6	0.8550(6)	0.3708(4)	0.1175(4)	0.017(1)	1
O7	0.1495(6)	0.5424(4)	0.1666(4)	0.019(1)	1
O8	0.5142(6)	0.2906(4)	0.1230(4)	0.016(1)	1
O9	0.5239(7)	−0.1223(4)	0.0132(4)	0.016(1)	1
O10	0.1789(6)	0.0716(4)	0.1895(4)	0.019(1)	1
O11	0.6978(7)	0.3036(4)	0.3136(4)	0.022(1)	1
O12	0.3805(6)	0.6911(4)	0.0938(4)	0.015(1)	1
O13	0.5345(7)	0.4968(4)	0.2155(4)	0.023(1)	1
O14	0.3067(7)	−0.3327(4)	0.3142(4)	0.016(1)	1
O15	0.3297(8)	0.7942(4)	0.4872(4)	0.025(2)	1
O16	0.1023(7)	−0.1163(4)	0.3141(5)	0.026(2)	1
K1	0.9829(2)	0.1664(1)	0.9955(1)	0.0220(4)	1
K2	0.1597(2)	0.3051(2)	0.2646(2)	0.0290(5)	1
K31	0.1769(4)	0.3425(4)	0.7266(3)	0.0266(8)	0.587(8)
K32	0.1543(9)	0.2955(7)	0.7160(5)	0.0266(8)	0.293(6)
K41	0.2448(8)	0.1122(5)	0.5152(3)	0.028(1)	0.46(1)
K42	0.304(2)	0.0781(11)	0.5093(8)	0.028(1)	0.189(8)
Kc1	0.4481(9)	0.5149(6)	0.5125(6)	0.054(2)	0.382(7)
Oc1	0	0.5	0.5	0.035(3)	0.40(2)
Oc2	−0.074(3)	0.476(1)	0.431(2)	0.035(3)	0.34(1)
Oc3	0.139(3)	0.345(2)	0.485(2)	0.035(3)	0.26(1)

Fig. 3. The crystal structure of $K_2SmAlSi_4O_{12} \cdot 0.375H_2O$ projected along [0 1 0]. Sm-polyhedra are shown in black, Si,Al-tetrahedra are colored white/gray.

Table 3
Relative coordinates and equivalent thermal parameters of atoms in the structure of $K_2SmAlSi_4O_{12} \cdot 0.375H_2O$.

Atom	x	y	z	U_{eq}	Occupancy
Sm	0.269409(4)	0.28655(1)	0.249234(7)	0.00698(5)	1
K1	0.80683(3)	−0.00478(9)	0.02651(5)	0.0247(2)	1
K2	0.96363(5)	0.2429(2)	0.03966(10)	0.0516(5)	1
Si1	0.16500(3)	0.53133(7)	0.00553(5)	0.0079(2)	1
Si2	0.34086(2)	−0.02051(7)	0.20881(5)	0.0074(2)	1
Si3	0.11823(2)	0.14349(7)	0.15898(4)	0.0072(2)	1
Si4	0.06149(3)	0.26467(8)	−0.07844(5)	0.0082(2)	1
Al	0.07152(3)	−0.19023(9)	0.22761(5)	0.0075(2)	1
O1	0.27804(7)	−0.0165(2)	0.1990(1)	0.0099(5)	1
O2	0.08890(9)	0.1409(2)	0.0296(1)	0.0183(6)	1
O3	0.32839(8)	0.2110(2)	0.4277(1)	0.0136(6)	1
O4	0.21190(8)	0.3699(2)	0.0699(1)	0.0145(6)	1
O5	0.38958(7)	−0.1498(2)	0.3082(1)	0.0127(5)	1
O6	0.36291(7)	0.1906(2)	0.2348(1)	0.0122(6)	1
O7	0.07225(8)	0.1458(2)	−0.1573(1)	0.0146(6)	1
O8	0.09519(7)	0.4596(2)	−0.0505(2)	0.0160(6)	1
O9	0.18737(7)	0.0841(2)	0.2249(1)	0.0123(5)	1
O10	0.07542(8)	0.0140(2)	0.1750(2)	0.0165(6)	1
O11	−0.00816(8)	0.3059(2)	−0.1278(2)	0.0157(6)	1
O12	0.33097(8)	−0.0963(2)	0.0973(1)	0.0146(6)	1
O13	0	0.212(4)	0.25	0.049(3)	0.22(2)
O14	0.0193(8)	0.270(2)	0.261(1)	0.049(3)	0.26(1)

C-centering were detected in the data. In a previous study, by contrast, the structure of a similar compound was resolved in the space group $P2_1/n$ [17]. Additional X-ray powder investigation showed that KGd-containing aluminosilicates from Ni and Cu containers are identical and belong to the space group $C2/c$. The KGd and KSm aluminosilicates are isostructural.

The crystal structure of the KSmAl compound is shown in Fig. 3 and refined atomic coordinates are given in Table 3. Anharmonic contributions to the displacement of K2 were refined up to fourth order in KGd alumosilicate. The aluminosilicate layers are the same in both structures and consist of double layers of Si- and Al-tetrahedra, forming four- and six-membered rings (Fig. 4). The layers are connected by columns of edge-shared 7-fold coordinated Sm or Gd polyhedra.

In the *C*-centered cell there is one polyhedral position of Sm or Gd in KSmAl or KGdAl silicate, respectively, with $\langle Sm{-}O \rangle = 2.416$ Å and $\langle Gd{-}O \rangle = 2.397$ Å. The two types of polyhedra Gd_1 and Gd_2 in [17] have the same average distance, $\langle Gd{-}O \rangle = 2.396$ Å.

There are two types of K- polyhedra in the *C*-centered structure of the KGdAl silicate: 8-fold and 9-fold coordinated K1 and K2 polyhedra with K1–O=2.726–3.476 Å and K2–O=2.826–3.453 Å, respectively, while in [17] there are 4 different types of K-coordination polyhedra. The situation is similar with tetrahedra, but variations in the interatomic distances are small: Al–O=1.719–1.752 Å and Si–O=1.598–1.659 Å, while in [17] Al–O=1.712–1.759 Å and Si–O=1.576–1.663 Å. In the KSmAl compound K1–O=2.827–2.346 Å and K2–O=2.720–3.367 Å, while aluminum and silicate tetrahedra have the following dimensions: Al–O distances vary from 1.718 to 1.751 Å and Si–O distances vary from 1.598 to 1.659 Å.

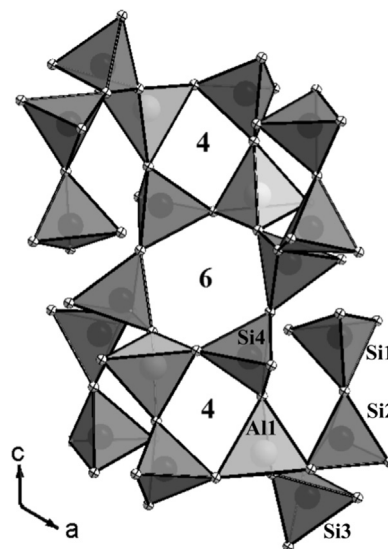**Fig. 4.** The $AlSi_4O_{12}$ layer in KSmAl and KGdAl silicates projected along [0 1 0]. Si and Al atoms are represented by dark and white spheres, respectively. Four- and six-membered rings are indicated.

The differences in the values of some interatomic distances and cell parameters of the KGd and KSm aluminosilicates (Table 1) correspond to the lanthanide contraction.

A structurally analogous compound of $Rb_2YGaSi_4O_{12}$ can be found in the literature (ICSD no. 173279) [18]. It was described in the space group $I2/a$ that is a different setting of $C2/c$. By degree of homogeneity, all phases of this section are suited best for group $C2/c$ ($I2/a$).

4.3. KYb silicate, $K_4Yb_2Si_8O_{21}$

Synthesized transparent colorless crystals with dimensions of less than 0.5 mm were examined under a binocular microscope. This optical inspection revealed anisotropy in accordance with monoclinic symmetry that was confirmed by crystal structure refinement in space group $C2/c$.

A sample of 0.35 mm × 0.16 mm × 0.10 mm in dimensions was chosen for the structural studies. The experimental data and the refinement conditions are listed in Table 1, whereas final crystallographic coordinates and thermal parameters of atoms and interatomic distances are reported in Tables 4 and 5, respectively.

A general view of the structure is shown in Fig. 5a and b. A characteristic feature of this structure are paired Yb-octahedra (Fig. 6). The structure of the Si_8O_{21} unit is shown separately (Fig. 7). It is formed of rings of six (a, b, c, a′, b′, c′), and four (a, a″, c″, c′) tetrahedra united via armstrongite-type bands, but with a tetrahedral orientation other than those given in [19,20]. Additional connection of sixfold rings via silicate dimers dd' becomes possible and results in two seven-fold rings that have a, b, d, d′, b″, a″ tetrahedra in common and are closed by either a c′ or c″ tetrahedron which is associated with a six-fold ring (Figs. 7 and 9). The six-fold and seven-fold rings are arranged such that they form an uninterrupted channel along the c-axis (Fig. 8) with the distance ~2.95 Å between the central oxygen atoms. A composition of this tubular unit formed by two six-fold Si_6O_{16} rings and two Si_2O_5 silicate dimers corresponds to the sum of Si_8O_{21} in agreement with the results of X-ray analysis.

The Yb atoms are coordinated by centrosymmetric pairs of octahedra linked via the shortened O1–O1 edges (2.233 Å). These octahedra are distorted due to a mutual repulsion of the Yb atoms. This explains, in particular, an elongation of Yb–O1 bonds and a deviation of O–Yb–O1 angles from 90° ($\angle O2YbO1 = 102°$, $\angle O1YbO1 = 76.2°$). Pairs of octahedra fulfill a dual role: They provide for the rigidity of tetrahedral chains and connect tubes of silicate anions, thus forming a mixed framework. All Si–O bonds involving atoms from the coordination environment of Yb are

Table 4
Relative coordinates and equivalent thermal parameters of atoms in the structure of $K_4Yb_2Si_8O_{21}$.

Atom	x	y	z	U_{eq}
Yb	0.11261(1)	−0.02528(1)	0.02389(1)	0.00728(6)
K1	0.15594(7)	−0.16157(7)	−0.1898(1)	0.0188(2)
K2	0.37904(8)	0.1500(1)	−0.0001(1)	0.0335(3)
Si1	0.09107(7)	−0.11966(8)	0.2684(1)	0.0073(2)
Si2	0.06620(7)	−0.31985(9)	−0.0550(1)	0.0080(2)
Si3	0.36045(7)	−0.06877(9)	0.2005(1)	0.0097(2)
Si4	0.31241(7)	0.15871(8)	0.2318(1)	0.0077(2)
O1	0.0457(2)	−0.0591(2)	0.1247(3)	0.0115(5)
O2	0.2604(2)	−0.1104(2)	0.1663(3)	0.0167(6)
O3	0.1424(2)	0.0315(2)	−0.1085(3)	0.0126(5)
O4	0.0536(2)	−0.1885(2)	−0.0864(3)	0.0152(6)
O5	0.1958(2)	0.1318(2)	0.1462(3)	0.0121(5)
O6	0.3267(2)	0.2828(2)	0.1917(3)	0.0124(5)
O7	0	0.1892(3)	0.75	0.0103(7)
O8	0.3771(2)	0.1491(3)	0.3968(3)	0.0218(7)
O9	0.4572(2)	−0.1160(3)	0.3537(3)	0.0193(6)
O10	0.3690(2)	−0.1163(3)	0.0891(3)	0.0212(7)
O11	0.3692(2)	0.0693(2)	0.2020(3)	0.0118(5)

Table 5
Interatomic distances (Å) and valence angles (degree) in the structure of $K_4Yb_2Si_8O_{21}$.

| Distances				Average
Yb–O1	2.270(3)	Yb–O5	2.238(3)	2.233(3)
Yb–O4	2.203(3)	Yb–O3	2.178(3)	
Yb–O2	2.196(3)	Yb–O1[i]	2.314(3)	
O1–O1[i]	2.829(5)	O5–O1[i]	3.372(4)	3.158(4)
O3–O1[i]	3.166(4)	O1–O4	3.183(4)	
O1–O5	3.323(4)	O2–O3	3.151(4)	
O4–O3	3.126(4)	O5–O3	2.987(4)	
O1–O2	3.472(4)	O4–O2	3.008(4)	
O5–O2	3.018(4)	O4–O1[i]	3.262(4)	
Si1–O1	1.617(3)	Si1–O3[ii]	1.587(3)	1.626(3)
Si1–O6[iii]	1.636(3)	Si1–O7[i]	1.662(2)	
Si2–O4	1.578(3)	Si2–O8[iii]	1.610(3)	1.612(3)
Si2–O9[v]	1.625(3)	Si2–O10[iv]	1.637(3)	
Si3–O2	1.573(3)	Si3–O9	1.634(3)	1.617(3)
Si3–O10	1.627(3)	Si3–O11	1.634(3)	
Si4–O5	1.588(3)	Si4–O6	1.623(3)	1.621(3)
Si4–O8	1.621(3)	Si4–O11	1.652(3)	
Si1–Si1	2.890(2)	Si2–Si3	3.112(2)	3.062(2)
Si1–Si4	3.108(2)	Si2–Si3	3.154(2)	
Si2–Si4	3.194(2)	Si3–Si4	2.914(2)	
K1–O3	2.576(3)	K2–O6[vi]	2.828(3)	
K1–O5[viii]	2.632(3)	K2–O11	2.865(3)	
K1–O4[vii]	2.820(3)	K2–O5[vi]	2.936(3)	
K1–O4	2.852(3)	K2–O9[viii]	2.978(3)	
K1–O2[iv]	2.977(3)	K2–O7[vi]	3.074(3)	
K1–O10[iv]	3.071(3)	K2–O2[viii]	3.341(3)	
K1–O10	3.077(3)	K2–O10	3.383(3)	
Angles				Average
Si1[i]–O7–Si1[viii]	120.9(2)	Si3–O9–Si2[iv]	145.5(2)	141.5(2)
Si4–O6–Si1[viii]	145.0(2)	Si3–O10–Si2[iv]	150.2(2)	
Si4–O8–Si2[viii]	162.5(2)	Si3–O11–Si4	124.9(2)	

shortened. This suggests a stronger influence by the Si due to its larger charge and smaller size.

The $Yb–O_1$ bond is slightly elongated. This effect is due to the O_1 atoms being influenced by both Yb atoms. The average Yb–O distance (2.233 Å) corresponds to the bond length 2.2 Å in the structure of Yb_2O_3 [21]. Bond angles Si–O–Si are reduced around the atoms O_7 and O_{11} because corresponding silicate dimers close the octahedral edges. The average value of the Si–O–Si angle (141.5°) is slightly smaller than an equilibrium value for framework structures (145°). K atoms surrounded by seven oxygen atoms with K–O distances from 2.576 to 3.077 and from 2.828 to 3.383 Å for K1 and K2, respectively (Table 4), normally have little effect on the structural characteristics and are located in the cavities of a framework for charge compensation. The local valence balance calculation (Table 6) shows a strong underbonding of the K2 position (K2 receives 0.65 v.u. compared to K1 with 1.11 v.u.).

Hence, the structure of the studied compound is a mixed framework formed by tubular chains connected via paired Yb-octahedra.

4.4. Comparison of the crystal structures of studied silicates and aluminosilicates with the armstrongite structure

Armstrongite $CaZr(Si_6O_{15}) \cdot 3H_2O$ is a rock-forming mineral of ongonite rocks [24]. In the armstrongite structure Si-tetrahedra are arranged in sheets with four-(a, a″, c″, c′) and six-membered (a, b, c, a′, b′, c′) rings (Fig. 9a). These sheets of $[Si_6O_{15}]^{6-}$ composition are connected to ZrO_6 octahedra and constitute the silicate anion of armstrongite. The four- and six-membered ring condensation yields the armstrongite-like sheets with derivative eight-membered rings (Fig. 10). We have observed that the structural units of silicates and
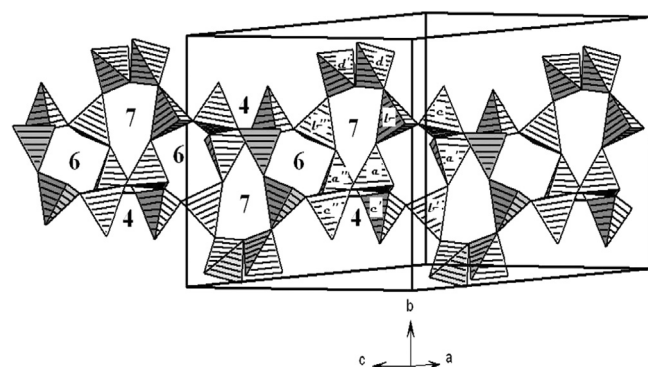
a

b
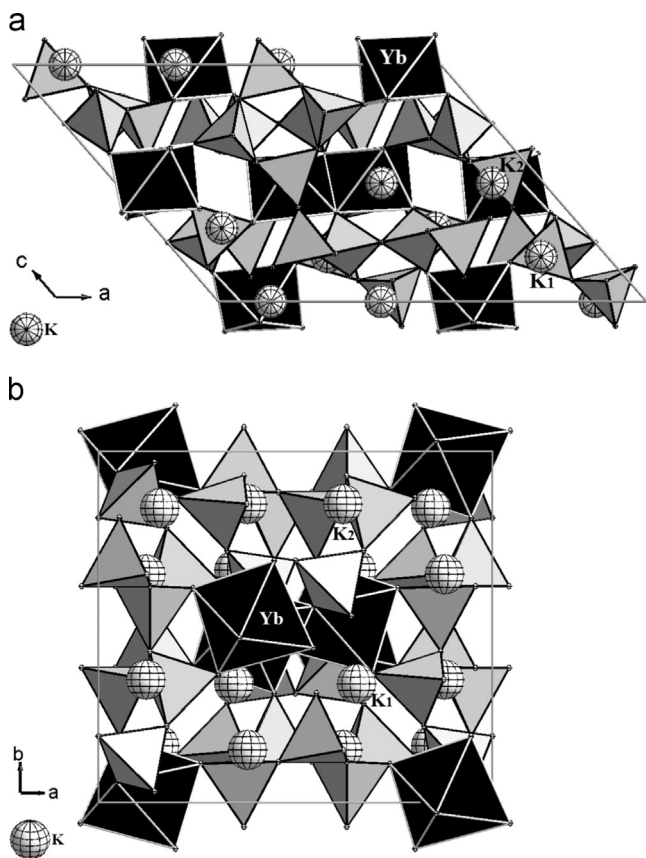
Fig. 5. (a) The crystal structure of $K_4Yb_2Si_8O_{21}$ projected along [0 1 0]. Yb-polyhedra are shown in black, Si-tetrahedra are colored white. (b) The crystal structure of $K_4Yb_2Si_8O_{21}$, projected along [0 0 1]. Yb-polyhedra are shown in black, Si-tetrahedra are white.
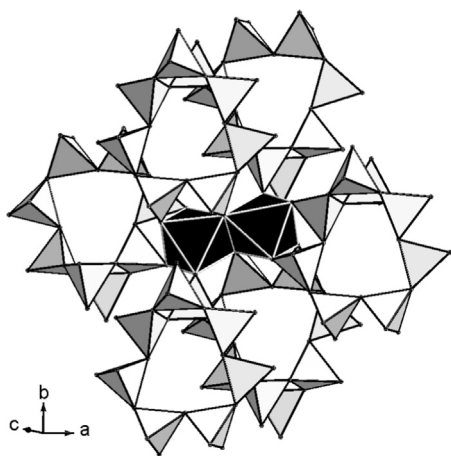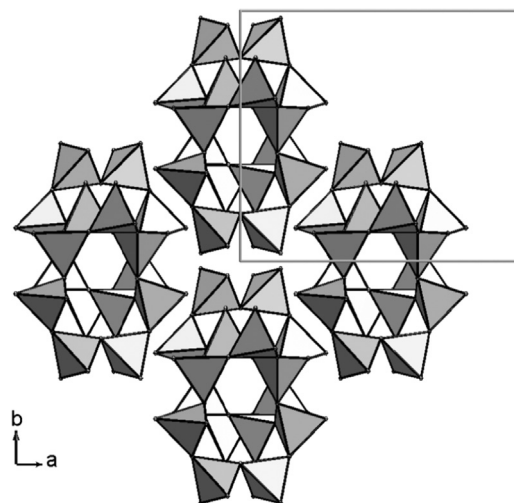

Fig. 6. Tubes joined with coupled octahedra in $K_4Yb_2Si_8O_{21}$. Yb-polyhedra are shown in black, Si-tetrahedra are white.

Fig. 7. Tubes of tetrahedral rings in the crystal structure of $K_4Yb_2Si_8O_{21}$. Four-, six-, and seven-membered rings are indicated.


Fig. 8. A fragment of the structure of $K_4Yb_2Si_8O_{21}$ projected along the c axis, showing Si_8O_{21} structural units.

aluminosilicates studied here can be derived from the armstrongite structure.

It appears that under crystallization the silicate anion primarily adjusts to the cation component, thus enhancing its stability. Stability is achieved by Si–O structural units of four-fold and six-fold rings; and even deviating units often can be represented as their derivatives. While analyzing a new structure $K_4Yb_2(Si_8O_{21})$, it was found that the tubes are formed by armstrongite-like bands of alternating six-fold (a, b, c, a′, b′, c′) and four-fold (a, a″, c″, c′) rings which form new split seven-fold rings (Fig. 9b). In the structures of the studied aluminosilicates (KGdAl and KSmAl) alternating four-

(a, c′, a″, c″) and six-membered (a, b, c, a′, b′, c′) tetrahedral rings can be distinguished: Aluminum tetrahedra participate in their formation. This armstrongite-like tetrahedral arrangement is disturbed by the introduction of *REE*-polyhedra and breaking of eight-membered rings (Fig. 9c).

The other example is the layer in structures of the KSm and KTb silicates. The authors of a similar K-*REE* silicate structure consider its silicate anion to be the product of condensation of several types of silicate chains and subsequent distortions [13]. It must be noted that this motive may be distinguished in the structure $Na_3Al_3Si_3O_{12}$ [25], and its condensation through the other mica-like motive may cause the formation of a framework in the third dimension. The relationship of $Si_{12}O_{32}$ structural units with Si_6O_{15} can be revealed clearly by using the concept of condensation of rings rather than chains.

In our view, the structural unit of this structure is a derivative of the armstrongite-like tetrahedral framework produced by disconnection of silicate dimers in the way that every other eigth-fold ring becomes a twelve-fold ring (Fig. 10). Such a network is also observed in the structures of delyite–davanite $K_2(Zr,Ti)Si_6O_{15}$ with triclinic distorted rings, sazhinite $Na_3Ce(Si_6O_{15}) \cdot 6H_2O$, bementite $Mn_7(Si_6O_{15})(OH)_8$ and a series of synthetic compounds with a more symmetric form of the rings. The armstrongite-type silicate band is the basis of the layer in the structure of complex mineral yakovenchukite–(Y)-$K_3NaCaY_2[Si_{12}O_{30}](H_2O)_4$ [26].

Thus, the idealized motive of the armstrongite silicate anion (Fig.10) is the prototype of the structures of KSm and KTb silicates. In particular, their Si–O structural unit is formed from the silicate
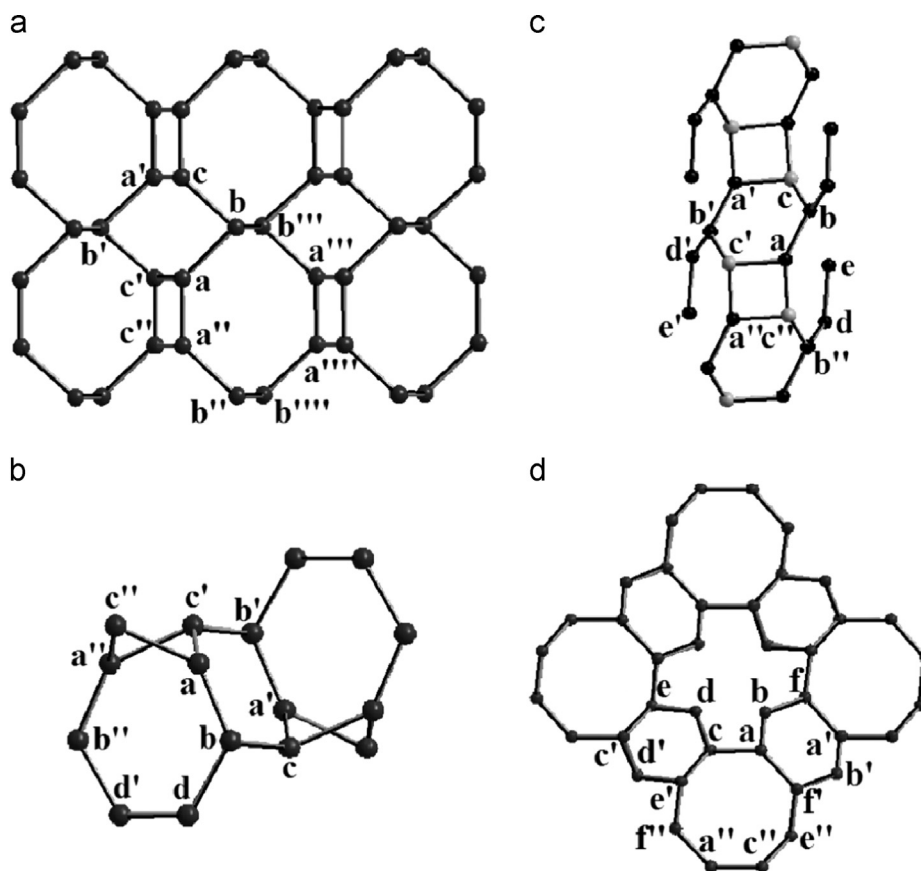
Fig. 9. Tetrahedral framework in the structures of the compounds (b–d) studied compared with armstrongite structure (*a*). (a) 3D nets corresponding to the tetrahedral framework in the structure of armstrongite; (b) 3D nodal representation of the Si-tetrahedral framework in the structure of $K_4Yb_2Si_8O_{21}$; (c) 3D nets of the Si–(black nets) and Al–(grey nets) framework in the structure of KSmAl and KGdAl silicates; (d) 2D nodal representation of the tetrahedral framework in KSm and KTb silicates.

Table 6
Bond valence calculation for $K_4Yb_2Si_8O_{21}$.

	O1	O2	O3	O4	O5	O6	O7	O8	O9	O10	O11	Sum
Yb	0.874	0.565	0.594	0.555	0.505	–	–	–	–	–	–	**3.093**
K1	–	0.101	0.300	0.297	0.257	–	–	–	–	0.156	–	**1.111**
K2	–	0.038	–	–	0.113	0.152	0.078[×2]	–	0.101	0.034	0.137	**0.653**
Si1	1.019	–	1.105	–	–	0.968	0.902[×2]	–	–	–	–	**3.994**
Si2	–	–	–	1.132	–	–	–	1.039	0.997	0.965	–	**4.133**
Si3	–	1.148	–	–	–	–	–	–	0.973	0.992	0.973	**4.086**
Si4	–	–	–	–	1.102	1.003	–	1.008	–	–	0.927	**4.040**
Sum	1.893	1.852	1.999	1.984	1.977	2.123	1.960	2.047	2.071	2.147	2.037	

[×2]—Doubled bond valence contribution for the calculation of anionic bond valence sums.
The analysis of the local valence balance wa carried out according to the method suggested by Brese and O'Keeffe (1991) [22] and Brown and Altermatt (1985) [23]. That is the valence, v_{ij}, of a bond between two atoms, *i* and *j*, having bond length, d_{ij}, is derived from the equation $v_{ij} = \exp[(R_{ij} - d_{ij})/b]$, where R_{ij} is the bond-valence parameter specific of an atom pair.

layer of armstrongite by broken four-fold rings (Figs. 1 and 10), that result from the necessity of hosting large cations that occupy edge-sharing octahedra, in contrast to silicate units coexisting with small cations of the type Zr, Ti etc. The formula of the silicate anion obtained results from the addition of two atoms of oxygen from the broken eight-fold rings according to the scheme $2[Si_6O_{15}]^{6-} + 2O^{2-} = [Si_{12}O_{32}]^{16-}$.

5. Conclusion

Hydrothermally synthesized K-*REE* silicates contain silica-oxygen structural units of different types. The KTb and KSm silicates contain $Si_{12}O_{32}$ units of a single-layer type. The KSm and KGd aluminosilicates are built of $AlSi_4O_{12}$ units of a double-layer type, whereas the KYb silicate contains a new tubular type of Si_8O_{21} unit, which has an average Si–O–Si angle similar to that of the framework silicates. The occurrence of pairwise edge sharing *REE* coordination octahedra is a remarkable feature of the KTb, KSm, KYb and KNd silicates [12,13]. Edge-sharing of two octahedra is observed for *REE*-containing silicates only. It should be emphasized that metal – oxygen octahedra in similar silicate structures form infinite chains or layers [27]. Our structures differ from the tubular chains in the structures of natural and synthetic silicates reviewed in [27] by a lower ratio of octahedral cations per Si. This may explain the absence of octahedral chains in favour of edge-sharing pairs of octahedra. Moreover, the silicate anion $(Si_{12}O_{32})^{16-}$ in KSm and KTb silicates can be related to the silicate layer of armstrongite $(Si_6O_{15})^{6-}$. It may result from the breaking of four-fold rings, which is caused by the necessity of hosting large cations that occupy the edge-sharing octahedra.
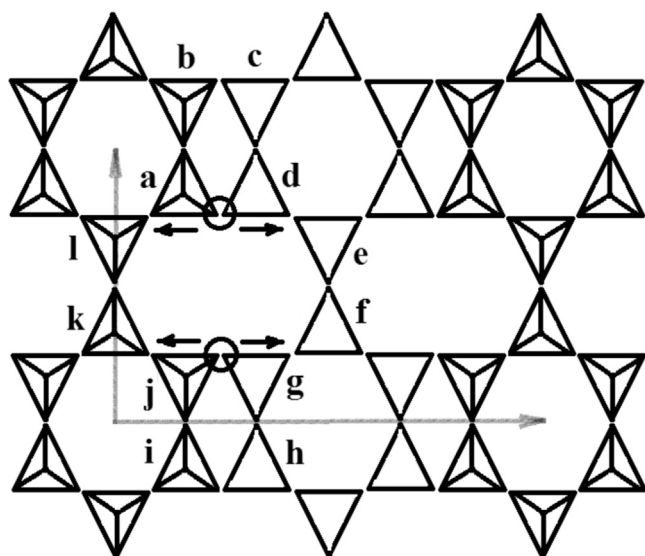
Fig. 10. Scheme of transformation of the idealized armstrongite-like tetrahedral layer in the process of [Si$_{12}$O$_{32}$] silicate anion formation. The apexes of the tetrahedra of broken rings are designated by circles and the trend of displacement of apexes is indicated by arrows. The corresponding tetrahedra are designated by the same symbols as in Fig. 1.

The new type of KYb-silicate mixed framework structure can also be derived from the armstrongite structure.

Acknowledgments

References

[1] V. Taroev, J. Göttlicher, H. Kroll, A. Kashaev, L. Suvorova, H. Pentinghaus, H. Bernotat-Wulf, U. Breit, V. Tauson, V. Lashkevich, Eur. J. Miner 20 (2008) 635–651.
[2] R.K. Rastsvetaeva, S.M. Aksenov, V.K. Taroev, Crystal. Reps. 55 (2010) 1041–1049.
[3] S.M. Aksenov, R.K. Rastsvetaeva, V.A. Rassylov, N.B. Bolotina, V.K. Taroev, V.L. Tauson, Micropor. Mesopor. Mater 182 (2013) 95–101.
[4] A.J.M. Duisenberg, J. Appl. Crystallogr. 25 (1992) 92–96.
[5] A.J.M. Duisenberg, L.M.J. Kroon-Batenburg, A.M.M. Schreurs, J. Appl. Crystallogr. 36 (2003) 220–229.
[6] A.M.M. Schreurs, X. Xian, L.M.J. Kroon-Batenburg, J. Appl. Crystallogr. 43 (2010) 70–82.
[7] L.J. Farrugia, J. Appl. Crystallogr. 32 (1999) 837–838.
[8] V. Petricek, M. Dusek, L. Palatinus, Jana 2006. The Crystallographic Computing System, Institute of Physics, Praha, Czech Republic, 2006.
[9] G.M. Sheldrick, SADABS. Version 2.01, Bruker AXS Inc., Madison, WI, 2004.
[10] G.M. Sheldrick, Acta Crystallogr. A 64 (2008) 112–122.
[11] F. Liebau, Structural Chemistry of Silicates: Structure, Bonding, and Classification, Springer-Verlag, Berlin, Heidelberg, New York, Tokyo, 1985.
[12] D. Ananias, M. Kostova, F.A.A. Paz, A.N.C. Neto, R.T. De Moura, O.L. Malta, L.D. Carlos, J. Rocha, J. Am. Chem. Soc. 131 (2009) 8620–8626.
[13] S.M. Haile, B.J. Wuensch, T. Siegrist, J. Solid State Chem. 148 (1999) 406–418.
[14] D.Y.u. Pushcharovskii, A.M. Dago, E.A. Pobedimskaia, N.V. Belov, Dokl. Akad. Nauk SSSR 258 (5) (1981) 1111–1114.
[15] V. Kahlenberg, T. Manninger, Acta Crystallogr E70 (2014) i11. http://dx.doi.org/10.1107/S1600536814001470.
[16] A.P. Zorina, E.L. Belokoneva, O.V. Dimitrova, Kristallografia 59 (1) (2014) 41–45.
[17] S.M. Aksenov, R.K. Rastsvetaeva, N.B. Bolotina, V.K. Taroev, in: Proceedings of the 14th international meeting "Order, Disorder and Properties of Oxides" ODPO-14, Rostov-on-Don, 2011, pp. 9-11 (in Russian).
[18] C.S. Lee, Y.C. Liao, J.T. Hsu, S.L. Wang, K.H. Lii, J. Inorg. Chem. 47 (2008) 1910–1912.
[19] A.A. Kashaev, A.N. Sapozhnikov, Sov. Phys. Crystallogr. 23 (1987) 539–542.
[20] A.A. Kashaev, Dokl. Akad. Nauk SSSR 293 (6) (1987) 1468–1470.
[21] I. Narai–Sabo, Inorganic Crystal Chemistry, Publ. (Sect. H), Academy of Science, Budapest, Hungary, 1969.
[22] I.D. Brown, D. Altermatt, Acta Crystallogr. B41 (1985) 244–247.
[23] N.E. Brese, M. O'Keeffe, Acta Crystallogr. B47 (1991) 192–197.
[24] V.I. Kovalenko, Petrology and Geochemistry of Rare Metal Granitoids, Nauka, SB Novosibirsk (1977) 204 (in Russian).
[25] K.G. Ragimov, M.I. Chiragov, N.M. Mustafaev, K.S. Mamedov, Dokl. Akad. Nauk SSSR 242 (1978) 839–841 (in Russian).
[26] S.V. Krivovichev, Y.A. Pakhomovsky, G.Y. Ivanyuk, J.A. Mikhailova, Y.P. Men'shikov, T. Armbruster, E.A. Selivanova, N. Meisser, Am. Miner. 92 (8-9) (2007) 1525–1530.
[27] I.V. Rozhdestvenskaya, S.V. Krivovichev, Crystallogr. Rep. 56 (2011) 1007–1018.